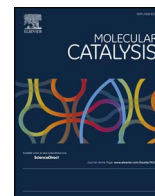




Contents lists available at ScienceDirect

Molecular Catalysis

journal homepage: www.elsevier.com/locate/mcat

Ceria-samarium binary metal oxides: A comparative approach towards structural properties and soot oxidation activity

Anjana P Anantharaman^a, Geethu J^a, Mohammed Rishab P^a, Hari Prasad Dasari^{a,*}, Jong-Ho Lee^{b,**}, Harshini Dasari^c, G Uday Bhaskar Babu^d

^a Chemical Engineering Department, National Institute of Technology Karnataka, Mangalore 575025, India

^b High-Temperature Energy Materials Research Center, Korea Institute of Science and Technology, Hwarangno 14-gil 5, Seongbuk-gu, Seoul 136-791, South Korea

^c Chemical Engineering Department, Manipal Institute Technology, Manipal Academy of Higher Education (MAHE), Manipal 576104, India

^d Chemical Engineering Department, National Institute of Technology Warangal, Warangal 506004, India

ARTICLE INFO

Keywords:

Ceria-samarium
Solid solution
Bi-phase
Band gap energy
Fluorite structure
Soot oxidation

ABSTRACT

Binary metal oxides of CeO₂-Sm₂O₃ (CS_x, x varies from 10 to 90 mol%) along with pure CeO₂ and Sm₂O₃ were synthesised successfully by the EDTA-Citrate method. From XRD, Raman spectroscopy and UV-vis DRS results, the whole composition of metal oxides exist in three phases: (fluorite phase (F) (CS10-CS30), bi-phase (fluorite (F) + cubic (C)) (CS30-CS90) and cubic phase (C) (Sm₂O₃)). For CS_x samples, the calculated band gap energy values obtained from the UV-vis DRS results were in between 3.0–5.1 eV and fluorite phase samples (CS10–CS30) displayed lower band gap energy values (3.04–3.07 eV) than compared to the samples in other phases. Similarly, from XPS analysis, fluorite phase samples (CS10–CS30) showed higher surface oxygen vacancy concentration than compared to samples in other phases. Catalytic activity for soot oxidation is carried out on CS_x samples, and the T₅₀ temperature is in between 480–540 °C. Fluorite phase samples (CS10 CS30) showed higher surface area, lower degree of agglomeration, lower band gap energy, higher oxygen vacancy concentration and better catalytic activity for soot oxidation. Among all the CS_x samples, CS10 sample displayed highest surface area (38 m²/g), lowest degree of agglomeration (0.36), lowest band gap energy (3.04 eV), highest oxygen vacancy concentration (64%) and highest soot oxidation activity (T₅₀ = 480 °C). The order of the soot oxidation activity of CS_x samples followed the same trend of band gap energy values.

1. Introduction

Application of catalysts predominantly in soot oxidation reaction manifests the ability to exchange oxygen during the reaction by improved rate of lattice oxygen interaction with soot owing to active oxygen participation. However, poor oxygen diffusion in the un-catalysed reaction is mainly because of the absence of intermediate steps since gaseous oxygen is directly reacted with soot [1]. Nano-size ranged particle demonstrates enhanced activity by increasing defect density and thus promoting active sites for catalytic reactions [2]. Ceria (CeO₂) is a promising catalyst attributable to its facile Ce⁴⁺/³⁺ redox cycles along with high oxygen storage/release capacity (OSC). Even with a minor addition of dopant to CeO₂ the catalytic activity of the material advances substantially [2]. Suitable addition of trivalent dopant into CeO₂ host lattice enriches oxygen vacancy as far as a solid solution is established [3]. The fluorite type open arrangement is highly adequate even with the dopant insertion without any structural deformation [4].

Tolerance of fluorite structure is high as far as the ionic size of both rare earth dopant (RE³⁺) and CeO₂ (Ce⁴⁺) are of the same range. Beyond the solubility limit, microdomains of cubic phase start growing within fluorite (F) matrix, which results in the hybrid structure [5]. Sm doping on CeO₂ lattice leads to mixed metal oxides with the difference in oxidation state and similarity in ionic radius and electronegativity between Ce⁴⁺ and Sm³⁺. Subsequently, structural stability of host ion is enhanced with the creation of oxygen vacancy by charge compensation mechanism. Some of the applications of Ce-Sm metal oxides are SOFC [6], CO oxidation [2], luminescence [7], oxygen sensors [8], benzyl alcohol oxidation [9], cyclohexane oxidation [10], light emitting diodes [11] etc.

Both stoichiometry and surface structure are vital issues in the catalytic activity of mixed metal oxides. In a system of Ce_{1-x}Sm_xO_{2-δ}, Artini et al. [6] and Vimal et al. [7] studied the structural variation over whole composition range and found that the phase boundary of F and C exist at x = 0.3 [6] and x = 0.2 [7], respectively. With the variation in

* Corresponding author.

** Corresponding author at: Energy Materials Research Center, Korea Institute of Science and Technology, Seoul, 136-791 South Korea.

E-mail addresses: energyhari@nitk.edu.in (H.P. Dasari), jongho@kist.re.kr (J.-H. Lee).

<https://doi.org/10.1016/j.mcat.2018.01.033>

Received 5 September 2017; Received in revised form 23 January 2018; Accepted 24 January 2018

2468-8231/© 2018 Elsevier B.V. All rights reserved.

the region of stable phase formation, oxygen vacancy also deviates since the condition of minimum energy diverges [5,6]. Since surface oxygen formation has a direct correlation with catalytic activity and even oxygen storage capacity of the material is enhanced with the higher availability of surface oxygen, detailed research on this aspect is necessary [12].

Variability in optical properties of rare earth metal oxides doped in host lattice has substantial influence in defect concentration, lattice strain and crystal symmetry [7]. The band gap energy of mixed metal oxides directly corresponds to excitation energy ligand to metal in an oxide. Band gap energy as a critical descriptor for catalytic activity in propene oxidation was studied using mixed metal oxides by Getsoian et al. [13], but the validity of their conclusion upon other ceria-based materials in catalytic activity is not yet extensively executed [13]. Also, the property that is key to enhance the catalytic activity of Ce-Sm metal oxide is not however solely discussed in detail.

This work emphasises the synthesis of binary metal oxide over a whole composition range of $\text{CeO}_2\text{-Sm}_2\text{O}_3$ using the EDTA-Citrate method. The synthesised samples were analysed using different characterisation techniques to find the structural property variation with dopant addition. The samples were tested for soot oxidation and the correlation of activity with different structural parameters was further analysed and discussed in depth.

2. Experimental details

2.1. Materials synthesis

Nano-crystalline binary metal oxide samples of $\text{CeO}_2\text{-Sm}_2\text{O}_3$ at varying composition were synthesised using the EDTA-Citrate method [15]. AR grade chemicals were used for the synthesis. Cerium nitrate hexahydrate and Samarium nitrate hexahydrate were used to synthesise the binary mixed metal oxides. Ammonium hydroxide solution was used to adjust the pH. The chelating agents used for this synthesis were Citric acid monohydrate and Ethylene Diamine Tetra Acetic acid (EDTA). Stoichiometric ratios of metal nitrates were added in such a way that the composition of Sm_2O_3 on CeO_2 varies from 0 to 100%. Synthesis procedure of EDTA-Citrate complexing method [14] was followed, and the black precursor solid obtained was oven dried at $150^\circ\text{C}/24\text{ h}$ followed by heat treatment at $350^\circ\text{C}/12\text{ h}$. Further calcination at $600^\circ\text{C}/5\text{ h}$ was carried to get the corresponding metal oxide samples. The obtained metal oxides, $\text{Ce}_x\text{Sm}_{1-x}\text{O}_{2-8}$ (where $x = 0\text{-}1$) was represented as CeO_2 , CS_x ($x = 10\text{-}90\text{ mol}\%$) and Sm_2O_3 , respectively.

2.2. Materials characterization

Raman spectra of the CS_x samples were obtained using Raman spectroscopy (Bruker: RFS 27 Model Raman spectrometer) with a charged-couple device (CCD) detector and a triple polychromator. Nd: YAG laser ($\lambda = 1064\text{ nm}$) was used as an excitation source with a laser power of 10 mW on the sample point. The CS_x samples were also characterized using X-ray diffraction (XRD), Transmission Electron Microscopy (TEM) and X-Ray Photoemission spectroscopy (XPS) techniques and the instrument details and the operating conditions were same as described in our earlier report by Anantharaman et al. [15]. The surface area of the CS_x samples was obtained using Surface area analyser Smart Sorb 92/93 model (Smart Instruments Company) operating on the principle of N_2 adsorption based on single point BET method. The sample holder along with the sample was placed in an oven at $150^\circ\text{C}/2\text{ h}$ to remove any moisture present in the sample before the test. Then, the tube was connected to the carrier gas line of the instrument to perform the test. Field Emission-Scanning Electron Microscopy (FE-SEM)/Energy Dispersive Spectroscopy (EDS) (CARL ZEISS SIGMA) was used to obtain the morphology and the composition of the CS_x samples. UV-vis NIR spectrometer (Cary 5000) was used to obtain the UV-vis Diffusive Reflectance Spectroscopy (DRS) measurements of the CS_x samples.

2.3. Soot oxidation activity

For soot oxidation activity measurements, standard soot (Printex U), (Orion Engineered Carbons) was used [16], and the experiments were conducted in tight contact condition by mixing it for 30 min with the catalyst in $4:1$ ratio in a mortar and pestle. The obtained mixture was preheated at $\sim 100^\circ\text{C}$ to remove any moisture content present. As described in the earlier reports [3,17], TGA instrument (TG/DTA 6300) was used to obtain the weight loss associated with the soot oxidation reaction [17]. The mixture (catalyst + soot) was kept in the sample holder of TGA instrument, and the change in weight was recorded with the increase in temperature (from 200 to 700°C) with a heating rate of $10^\circ\text{C}/\text{min}$ in the presence of air at a flow rate of $100\text{ ml}/\text{min}$ [17]. The reproducibility for the soot oxidation activity of each sample was performed to validate the results and the order of the catalytic activity.

3. Results and discussion

3.1. XRD analysis

Fig. 1(a) depicts the XRD patterns of CS_x sample calcined at $600^\circ\text{C}/5\text{ h}$

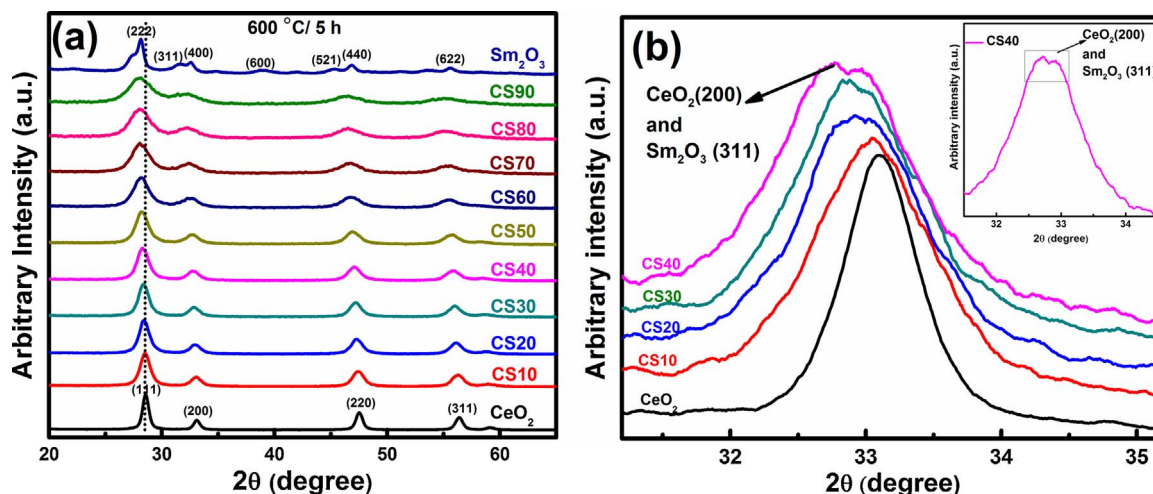


Fig. 1. (a) XRD pattern of CS_x samples calcined at $600^\circ\text{C}/5\text{ h}$ (b) XRD pattern corresponding to (111) peaks up to CS_{40} and peak splitting for CS_{40} sample (inset).

Download English Version:

<https://daneshyari.com/en/article/8916845>

Download Persian Version:

<https://daneshyari.com/article/8916845>

[Daneshyari.com](https://daneshyari.com)